

Yu-Lan Zhen, Guo-Hua Zhang\* and Kuo-Chih Chou

# Carbothermic Reduction of Titanium-Bearing Blast Furnace Slag

**Abstract:** The carbothermic reduction experiments were carried out for titanium-bearing blast furnace slag in Panzhihua Iron and Steel Company in argon atmosphere at high temperatures. The effects of reduction temperature, isothermal treatment time and carbon content on the formation of TiC were studied by X-ray diffraction (XRD) and scanning electron microscope (SEM). The XRD pattern results showed that  $\text{MgAl}_2\text{O}_4$  phase disappeared and the main phase of the reduced sample was TiC when the reduction temperature was higher than 1,773 K. The SEM pictures showed that the reduction rate of the titanium-bearing blast furnace slag could be increased by enhancing the temperature and the C content (carbon ratio  $\leq 1.0$ ). Furthermore, it was also found that TiC had the tendency of concentrating around the iron. The effects of additives such as Fe and  $\text{CaCl}_2$  on the formation of TiC were also studied in the present study.

**Keywords:** titanium-bearing blast furnace slag, carbothermic reduction, titanium carbide

DOI 10.1515/htmp-2014-0159

Received September 12, 2014; accepted March 10, 2015

## Introduction

Vanadium–titanium-bearing magnetite of Panzhihua, China, is a complex iron ore with the coexistence elements of vanadium and titanium. It accounts for more

than 90% of the titanium reserves in China. By the beneficiation process of the ore, titanomagnetite concentrates and ilmenite concentrates are produced [1, 2]. The titanomagnetite concentrates are used as the main materials for the blast furnace process in Panzhihua area now. In this process, most of the iron and partly of the vanadium can be reduced into the hot metal; however, almost all of the titanium remains in the slag, forming the high titanium bearing slag, which contains about 21–25% of  $\text{TiO}_2$ , and emission in every year is more than 3 million tons [3]. This slag is the considerable strategic resources and the precious wealth. There is no appropriate and economic method to deal with such slag so far. Titanium is very important and useful metal which is widely used in the aerospace and chemical industrial. Many countries regard the deposit of titanium as a strategic resource. China is abundant in titanium, accounting for about 48% of the world. However, the recovery ratio of the titanium is too low in the current smelting process of the vanadium titanomagnetite resource.

Over the past several decades, many works have been conducted on the mechanism and kinetics of the carbothermic reduction of titanomagnetite [4–11] and titanium-bearing blast furnace slag [12–15]. Li et al. [12, 13] researched the extracting Ti(C, N) from high-titanium slag, results of which confirm that the final products consist mainly of TiC in argon atmosphere and  $\text{TiC}_{0.3}\text{N}_{0.7}$  in nitrogen atmosphere. Feng et al. [14] described the preparation of TiC from  $\text{TiO}_2$  bearing blast-furnace slags from Panzhihua and indicated that the final obtained TiC-containing slag can be used in superior refractory materials. Li et al. [15] studied the carbonization (nitrogenation) for titanium-bearing blast furnace slag by plasma furnace. With the sample of slag being held in the plasma furnace at 1,973 K for 1 h, 92%  $\text{TiO}_2$  in the slag can be transformed into Ti(C,N) and the diameter of Ti(C,N) crystalline is more than 20  $\mu\text{m}$ . Although many works have been done, the recycling utilization of  $\text{TiO}_2$  bearing blast furnace slag still had some problems. All of these works were focused on the crystalline slags which were cooled in the air slowly after samples are reduced at different temperatures for

---

**\*Corresponding author: Guo-Hua Zhang**, State Key Laboratory of Advanced Metallurgy, University of Science and Technology Beijing, Beijing 100083, China; School of Metallurgical and Ecological Engineering, University of Science and Technology Beijing, Beijing 100083, China, E-mail: ghzhang\_ustb@163.com

**Yu-Lan Zhen:** E-mail: zhenzhen9545@126.com, **Kuo-Chih Chou:** E-mail: zhouguozhi\_sci@126.com, State Key Laboratory of Advanced Metallurgy, University of Science and Technology Beijing, Beijing 100083, China; School of Metallurgical and Ecological Engineering, University of Science and Technology Beijing, Beijing 100083, China

different times, and the crystalline phase containing spinel, akermanite–gehlenite and diopside and so on. Then the problem is that it is very hard to remove the crystalline phase even using acid leaching if extracting pure TiC from the treated slag, especially spinel, which is insoluble in both acid and alkali. If no crystalline phase is formed after high temperature treatment, it will be much easy to remove these glass phases. Therefore, the aim of the present study is to obtain the glass slags and to avoid the precipitation of spinel and other crystalline phase, and then find the best experimental conditions for carbothermic reduction.

## Experimental procedures

Chemical compositions of the titanium-bearing blast furnace slag were examined by the X-ray fluorescence (Shimadzu XRF-1800, current 140 mA, voltage 60 kV), which was presented in Table 1. Figure 1 shows the X-ray diffraction (XRD, conducted using a Cu-K $\alpha$  source) patterns of the slag. The main mineral phase of the titanium-bearing blast furnace slag is CaTiO<sub>3</sub>.

**Table 1:** Chemical composition of the titanium-bearing blast furnace slag (wt%).

Components	SiO <sub>2</sub>	CaO	TiO <sub>2</sub>	Al <sub>2</sub> O <sub>3</sub>	MgO	Fe <sub>2</sub> O <sub>3</sub>	Others
Content	23.64	28.06	24.45	11.39	7.58	1.40	3.48

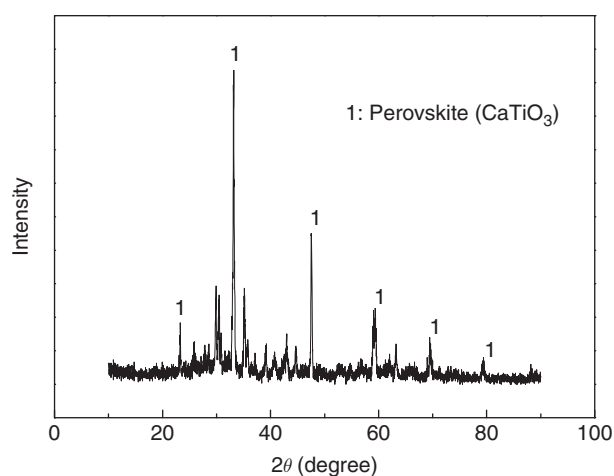


**Figure 1:** XRD patterns for titanium-bearing blast furnace slag in Panzhihua.

The titanium-bearing blast furnace slag and the graphite powder were mixed homogenously with the addition of the alcohol. By considering eqs (1) and (2), the mass ratios of C to slag in mixtures were set to be 7.75:100 (corresponding to the carbon molar ratio of 0.70), 9.69:100 (corresponding to the carbon molar ratio of 0.85), 11.63:100 (corresponding to the carbon molar ratio of 1.0), 13.03:100 (corresponding to the carbon molar ratio of 1.15), respectively.



Then the mixtures were dried to get rid of the alcohol at 393 K for 2 h. The powder was placed in an alumina crucible. Vertical tube furnace with silicon molybdenum as the heating element was used. The temperature was accurately controlled within  $\pm 1$  K by PID controller under a flowing argon atmosphere. The alumina crucible was put into the hot zone of the vertical tube furnace quickly when the furnace temperature reached the desired value. The isothermal reduction reactions at three different temperatures were studied, as 1,673, 1,773 and 1,873 K, respectively. The reaction time at each reaction temperature was 2, 4 and 6 h, respectively. The samples reduced at different temperatures for different times were cooled in the water quickly after the alumina crucibles were took out from the furnace. The reduced slags were examined by XRD and SEM (Mineral Liberation Analyzer, voltage 200 V to 30 kV) analyses to study its phase composition and morphology.

In addition, in order to obtain the percentage of total mass loss, each samples reduced at different temperatures for different times were also prepared again. But instead of quenching in water, these samples were took out from the furnace and cooled in the argon.

## Results

### Thermodynamic calculation

- (1) The main reactions probably occurred during the carbothermic treatment of titanium-bearing blast furnace slag are given as follows:

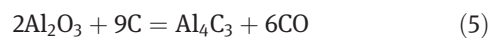


**Table 2:** Results of the thermodynamics calculation by FactSage6.0.

Equation	Reaction	$\Delta G^\theta$ (J/mol)	$T_{\text{start}}$ (K)
(1)	$\text{TiO}_2 + 3\text{C} = \text{TiC} + 2\text{CO}$	263,700–168.29 T	1,567
(3)	$\text{CaO} + 3\text{C} = \text{CaC}_2 + \text{CO}$	465,500–220.62 T	2,110
(4)	$\text{MgO} + \text{C} = \text{Mg} + \text{CO}$	486,830–193.36 T	2,518
(5)	$2\text{Al}_2\text{O}_3 + 9\text{C} = \text{Al}_4\text{C}_3 + 6\text{CO}$	685,500–349.51 T	2,265
(6)	$\text{SiO}_2 + 3\text{C} = \text{SiC} + 2\text{CO}$	594,950–332.15 T	1,792

**Table 3:** Activities of different components in the titanium-bearing blast furnace slag.

Components	$\text{SiO}_2$	$\text{CaO}$	$\text{TiO}_2$	$\text{Al}_2\text{O}_3$	$\text{MgO}$
$\alpha/(10^{-2})$	7.896	0.141	8.997	1.7502	1.487

The results of thermodynamics calculation by FactSage6.0 were given in Table 2. The activities of different components in titanium-bearing blast furnace slag are listed in Table 3. From Table 2, it could be indicated that eqs (3)–(5) would not occur, due to the initial reaction temperatures  $T_{\text{start}}$  are much higher than 1,873 K which is the highest treatment temperature of the present study. Considering that the activities of CaO, MgO and  $\text{Al}_2\text{O}_3$  are less than 1, the  $T_{\text{start}}$  will be even higher. The Gibbs free energy change of eqs (1) and (6) are given as follows:

$$\Delta G_1 = \Delta G_1^\theta + RT \ln \frac{(P_{\text{CO}}/P^\theta)^2 \cdot \alpha_{\text{TiC}}}{\alpha_{\text{TiO}_2} \cdot \alpha_{\text{C}}^3}$$

$$\Delta G_6 = \Delta G_6^\theta + RT \ln \frac{(P_{\text{CO}}/P^\theta)^2 \cdot \alpha_{\text{SiC}}}{\alpha_{\text{SiO}_2} \cdot \alpha_{\text{C}}^3}$$

In the molten slag, TiC and SiC exist as independent phase, so  $\alpha_{\text{TiC}} = 1$  and  $\alpha_{\text{SiC}} = 1$ ; CO occurred in the liquidus slag,  $P_{\text{CO}} \approx P^\theta$ ;  $\alpha_{\text{C}} = 1$ ;  $\alpha_{\text{TiO}_2} = 8.997 \times 10^{-2}$ ,  $\alpha_{\text{SiO}_2} = 7.986 \times 10^{-2}$ . So

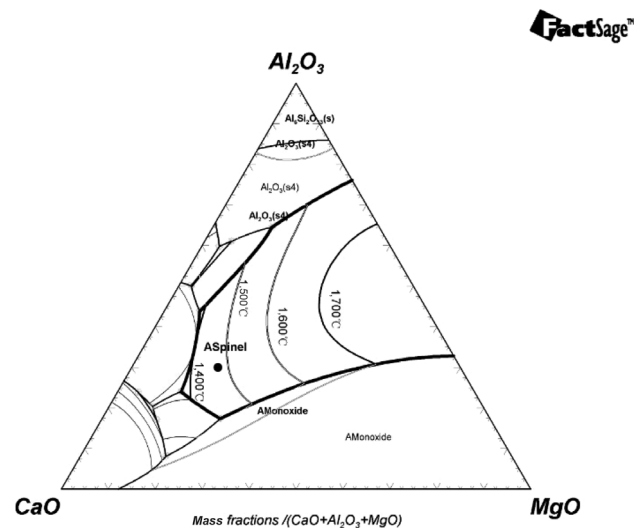
$$\Delta G_1 = \Delta G_1^\theta + RT \ln \frac{1}{\alpha_{\text{TiO}_2}}, T_{\text{start}1}' = 1,589 \text{ K} < 1,673 \text{ K}$$

$$\Delta G_6 = \Delta G_6^\theta + RT \ln \frac{1}{\alpha_{\text{SiO}_2}}, T_{\text{start}6}' = 1,912 \text{ K} > 1,873 \text{ K}$$

Therefore, C could only reduce  $\text{TiO}_2$  in the slag at the present reduction temperature.

- (2) After reduced, the mainly chemical compositions of slag are CaO, MgO,  $\text{Al}_2\text{O}_3$ ,  $\text{SiO}_2$  and TiC. TiC exists in the form of solid particles at the present reduction temperature. The other components form CaO-MgO- $\text{Al}_2\text{O}_3$ - $\text{SiO}_2$  slag system. The result of phase diagram

for CaO-MgO- $\text{Al}_2\text{O}_3$  system (constant  $\text{SiO}_2$  content) by FactSage6.0 was given in Figure 2. From Figure 2, it can be seen that the composition of completely reduced titanium-bearing blast furnace slag (the black spot in Figure 2) exists in the spinel phase when the temperature is less than 1,763 K. Therefore, if the temperature is lower than 1,763 K, spine will be formed as a thermodynamic stable phase, while it can be avoided at a higher temperature. Of course, in order to keep the phase composition at high temperature, the quenching is necessary. In the present work, it is completed by water quenching.

**Figure 2:** Phase diagram of CaO- $\text{Al}_2\text{O}_3$ -MgO system.

## The percentage of total mass loss

During the reduction of titanium-bearing blast furnace slag by graphite, the percentage of total mass loss ( $W$ ) was calculated by the following reaction formula, where  $w_t$  is the initial mass of the mixture:

$$W = \frac{w_0 - w_t}{w_0} \times 100\% \quad (7)$$

The changes of weight loss ratio with temperature and time are shown in Figures 3–9. Figures 3–5 show that in the case of the same temperature, the higher the carbon ratio ( $\leq 1.0$ ) is, the faster the reaction rate and the larger the maximum weight loss ratio will be; but when the carbon ratio was higher than 1.0, the maximum value of weight loss ratio decreased obviously, and the reaction rate also cannot increase any more with the increase of carbon ratio. Therefore, the carbon ratio of 1 is enough for the reduction reaction and the further increase of carbon ratio could not lead to the increases of reaction rate and the maximum weight loss ratio. When the carbon ratio is 1.15, the excess carbon could not participate into the reaction but only increase

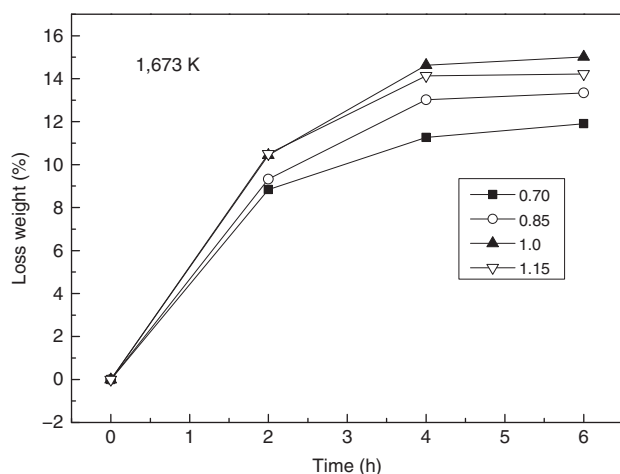


**Figure 3:** The percentage of total mass loss with different carbon ratios at 1,673 K.

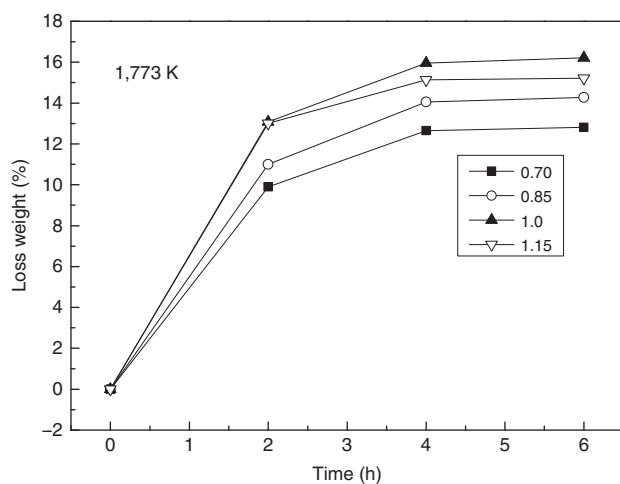


**Figure 4:** The percentage of total mass loss with different carbon ratios at 1,773 K.

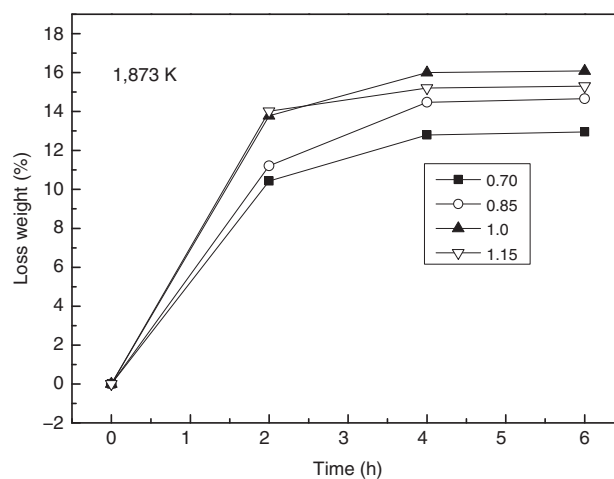


**Figure 5:** The percentage of total mass loss with different carbon ratios at 1,873 K.

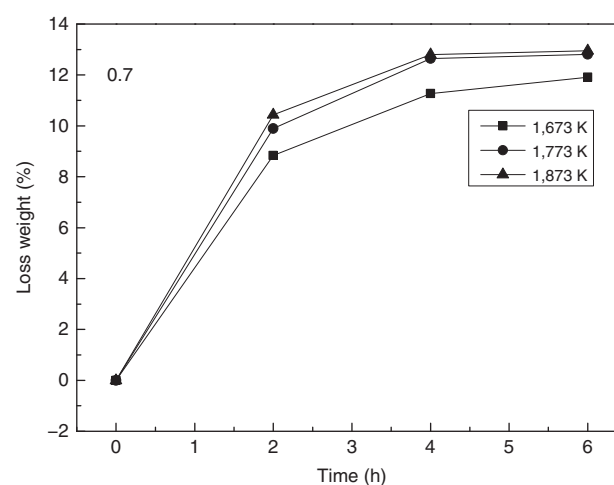


**Figure 6:** The percentage of total mass loss with carbon ratio of 0.7 at different temperatures.

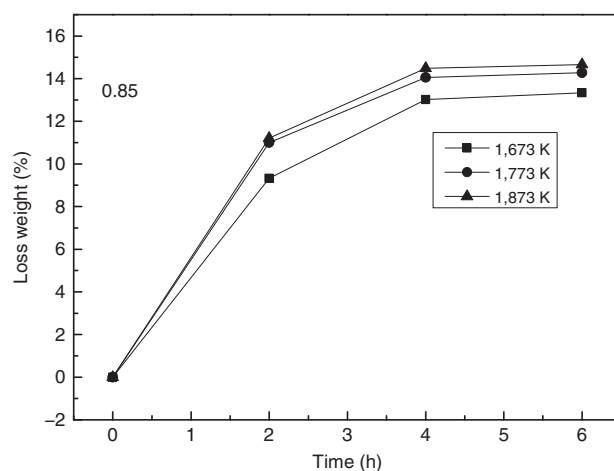


**Figure 7:** The percentage of total mass loss with carbon ratio of 0.85 at different temperatures.



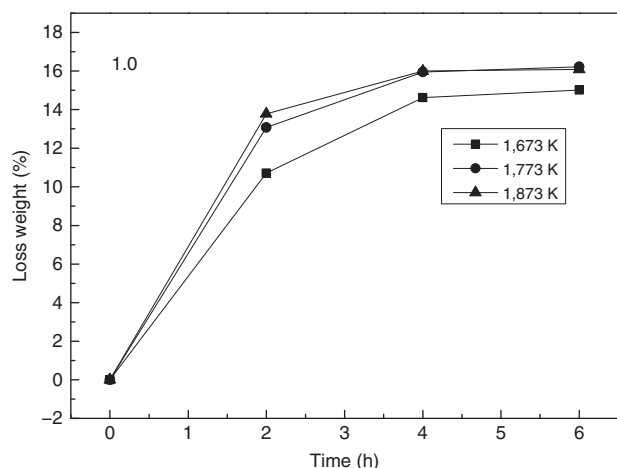


**Figure 8:** The percentage of total mass loss with carbon ratio of 1.0 at different temperatures.

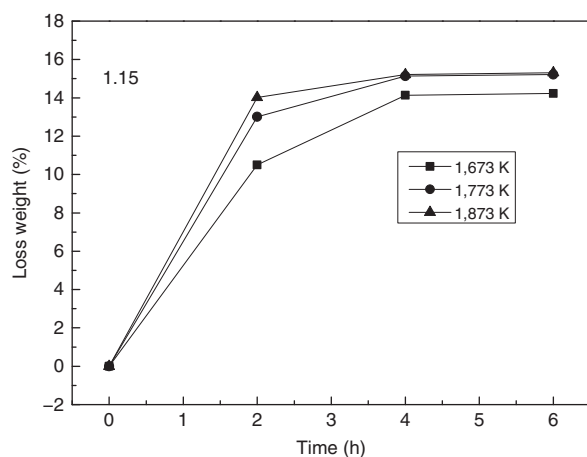


**Figure 9:** The percentage of total mass loss with carbon ratio of 1.15 at different temperatures

the initial mass  $w_0$ , subsequently, according to eq. (7), the maximum weight loss will decrease. Figures 6–9 show that the mass loss ratio is much larger when reacting at a higher reduction temperature from 1,673 to 1,773 K. However, as the temperature is higher than 1,773 K, both the reaction rate and the maximum value of weight loss ratio just had a negligible change. From these figures, it could also be seen that the reduction reaction could be finished when the reduction time is longer than 4 h.

## X-ray diffraction

In the case of 1,673 K, the XRD patterns of the samples reduced with different carbon ratios for 2 h are

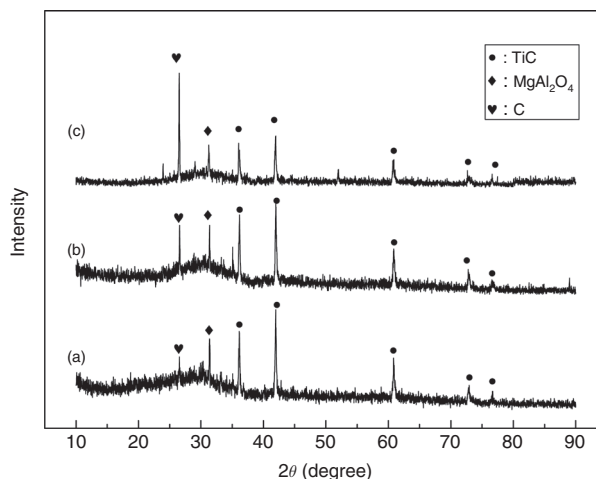


**Figure 10:** XRD results of reduced samples at 1,673 K, 2 h for different carbon ratios: (a) 0.7, (b) 0.85 and (c) 1.0.

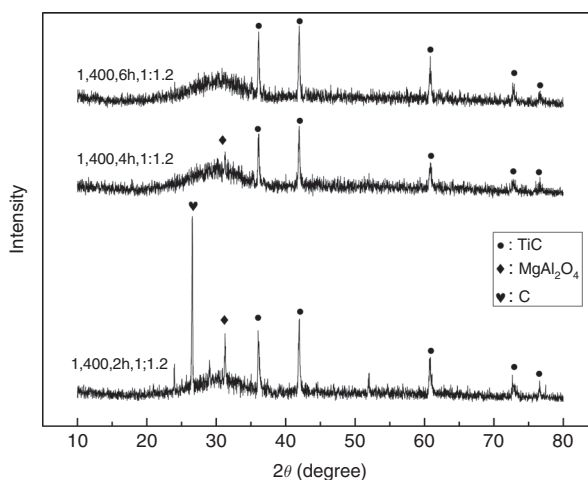


**Figure 11:** XRD results of reduced samples with carbon ratio of 1.0, at 1,673 K for different times: (a) 2 h, (b) 4 h and (c) 6 h.

presented in Figure 10. Figure 11 gives the XRD results of reduced samples for different reduction times with carbon ratio of 1.0, at 1,673 K. The XRD pattern results show that the main phases of the reduced samples at 1,673 K were TiC,  $\text{MgAl}_2\text{O}_4$  and C. From Figures 10 and 11, it can be seen that there was no obvious change in the main phases as increasing the carbon ration and reduction time at 1,673 K. But C phase gradually decrease with the increase of reduction time, and disappeared after being reduced for 4 h at 1,673 K (shown in Figure 11).

In the case of 1,773 K, the XRD patterns of the samples reduced with carbon ratio of 1.0 for different times are presented in Figure 12, and Figure 13 gives the XRD results of reduced samples with different

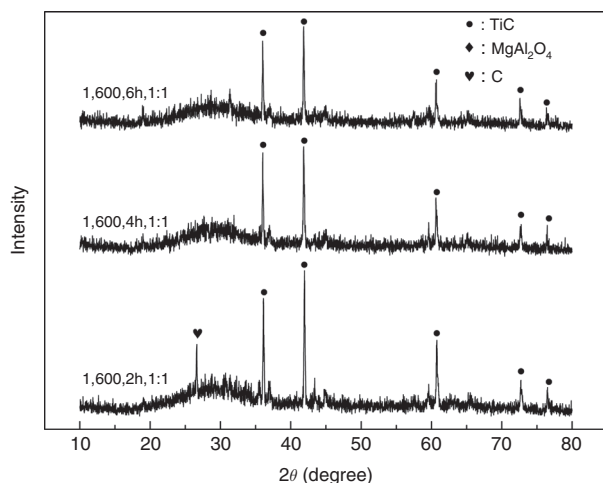


**Figure 12:** XRD results of reduced samples with carbon ratio of 1.0, at 1,773 K for different times: (a) 2 h, (b) 4 h and (c) 6 h.

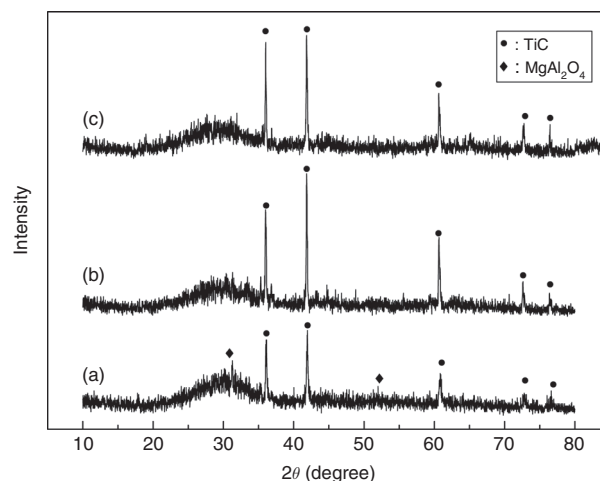


**Figure 14:** XRD results of reduced samples with carbon ratio of 1.0, for 4 h at different temperatures: (a) 1,673 K; (b) 1,773 K; (c) 1,873 K.

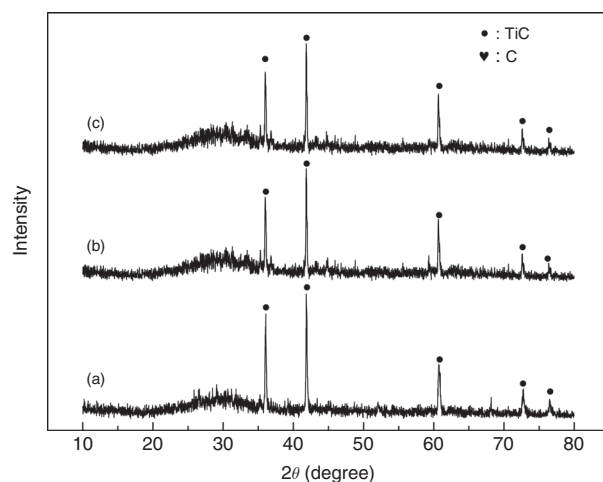


**Figure 13:** XRD results of reduced samples at 1,773 K, 4 h for different carbon ratio: (a) 0.7; (b) 0.85; (c) 1.0.

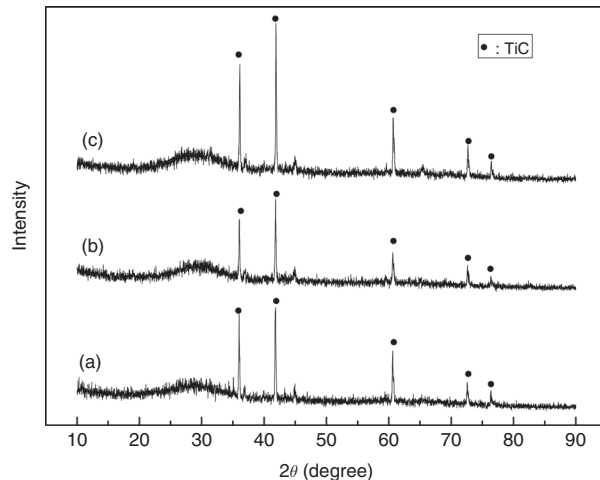


**Figure 15:** XRD results of reduced samples with carbon ratio of 1.0, 2 h, at 1,873 K for different additives: (a) 5 wt%  $\text{CaCl}_2$ ; (b) 5 wt% Fe; (c) none.

carbon ratios for 4 h. The XRD patterns results show that the main phases of the reduced sample at 1,773 K were TiC and C. It could also be seen that  $\text{MgAl}_2\text{O}_4$  phase disappeared after being reduced at 1,773 K, which means the main phase of the reduced sample was TiC when the reduction temperature is more than 1,773 K. It is also in accordance with the result of phase diagram (Figure 2).

In the case of 1,873 K, the XRD results of reduced samples with carbon ratio of 1.0, for 4 h at different reduction temperature are presented in Figure 14. The XRD patterns results show that the main phase of the

reduced sample was TiC when the reduction temperature more than 1,773 K. In addition, the effect of additives such as Fe and  $\text{CaCl}_2$  on the reduction was studied. The XRD results of reduced samples with carbon ratio of 1.0, 2 h, at 1,873 K for different additives are given in Figure 15. From Figure 15, the main phases of the samples reduced without or with additive were still TiC.

## The microstructure of the reduction product

Backscattered Electron Diffraction (BSED) images of the samples reduced for different carbon ratios and different

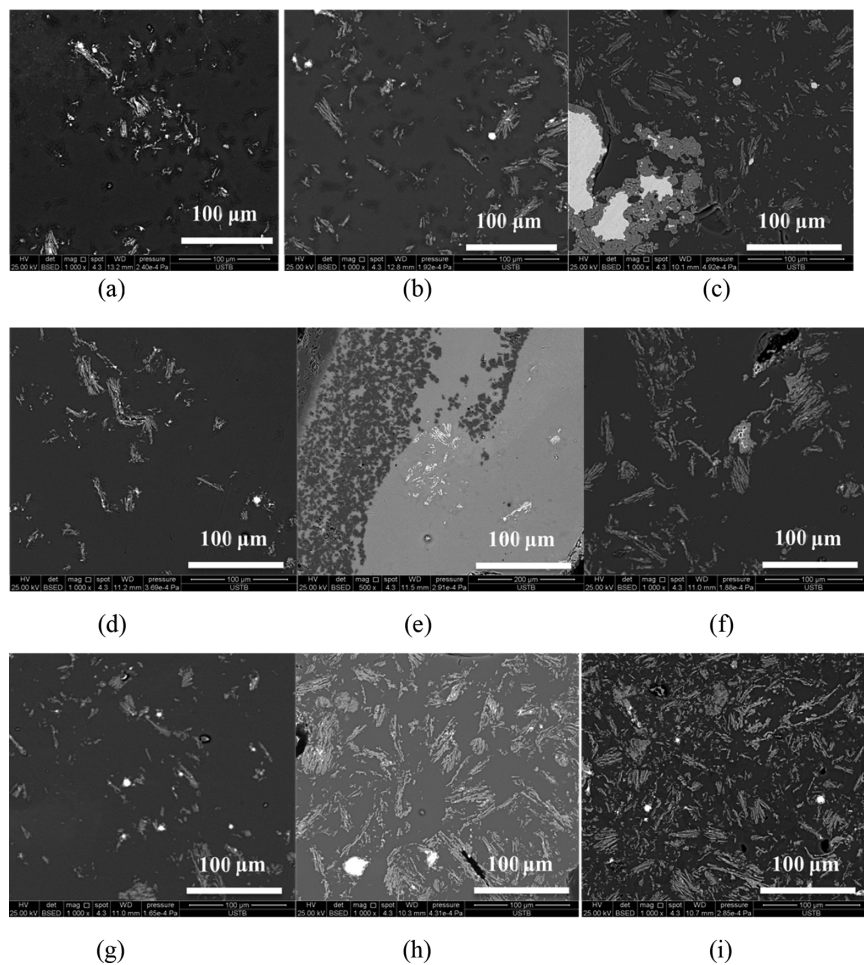


**Figure 16:** BSED images of the samples reduced with different carbon ratios for different times at 1,673 K: (a) 2 h, 0.7; (b) 2 h, 0.85; (c) 2 h, 1.0; (d) 4 h, 0.7; (e) 4 h, 0.85; (f) 4 h, 1.0; (g) 6 h, 0.7; (h) 6 h, 0.85 and (i) 6 h, 1.0.

reduction times at 1,673 K are shown in Figure 16(a)–(i). The BSED image reveals three distinct regions which appear as bright, light gray, dark gray, some black. In order to identify the phases, Energy Dispersive Spectrometer (EDS) analyses were performed at different regions as shown in SEM images of Figure 17(b)–(e). The region 1 consists of 86.50% Fe, which indicates that the bright phase is composed of Fe phase. The region 2 is made up of 78.96% Ti, and 11.68% C, which indicates that the light gray phase is mainly composed of TiC phase. The region 3 consists of many elements, such as 34.10% O, 25.29% Al, 20.88% Ca, 8.47% Si, 9.30% Ti, 1.96% Mg and so on, which implies that the dark gray phase is mainly incompletely reduced titanium-bearing blast furnace slag. The region 4 is made up of 30.23% O, 46.13% Al and 18.32% Mg, which indicates that the black phase is mainly composed of  $\text{MgAl}_2\text{O}_4$  phase.

BSED images of the samples reduced for different carbon ratios and different times at 1,773 K are shown in Figures 18(a)–(i). There are three distinct regions. Compared to 1,673 K, the black phase disappeared, which means the main phases of the products were TiC and Fe when the temperature was higher than 1,773 K.

BSED images of the samples reduced for different carbon ratios and different reduction times at 1,873 K are shown in Figure 19(a)–(i). There are also three distinct regions.

In order to enhance the conversion rate of TiC, about 5% of  $\text{CaCl}_2$  or Fe was added.  $\text{CaCl}_2$  was added for its strong ability of decreasing viscosity which is beneficial for the diffusion transport of titanium ion, while Fe is added to increase the nuclei of

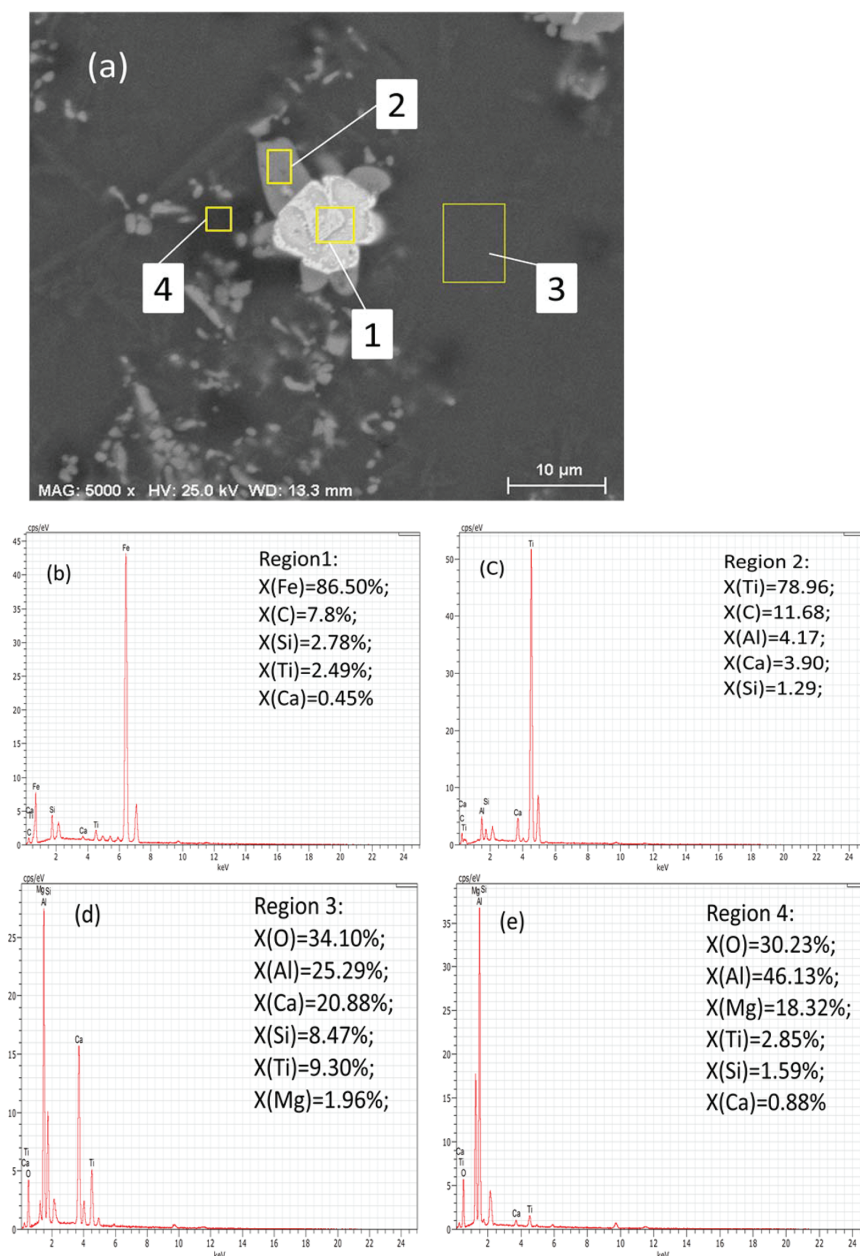


Figure 17: SEM image (a) of reduced sample at 1,673 K (with carbon ratio 0.85, 2 h) and EDS results of regions 1 (b), 2 (c), 3 (d) and 4 (e).

heterogeneous nucleation of TiC. BSED images of the samples reduced for carbon ratio of 1.0, 2 h, at 1,873 K for different additives are shown in Figure 20(a)–(c). The results show that the areas of TiC phase are larger by adding the additives, especially  $\text{CaCl}_2$ , which implies that the additives could be helpful for reaction. Furthermore, Fe and TiC were obviously found to be mixed together tightly from Figure 13(b), which may imply that the additive of Fe could be helpful for the nucleation of TiC.

## Discussion

- (1) From Figures 16(a)–(i), 17(a)–(i) and 18(a)–(i), it can be seen that more TiC could be produced by improving the C content and reaction time at each temperatures. That is, the reaction rate would be improved by increasing the C content (carbon ratio  $\leq 1.0$ ) and the degree of reduction would be enhanced by increasing reaction time. By comparing Figures 16, 17 and 18, the higher temperature is, the bigger than



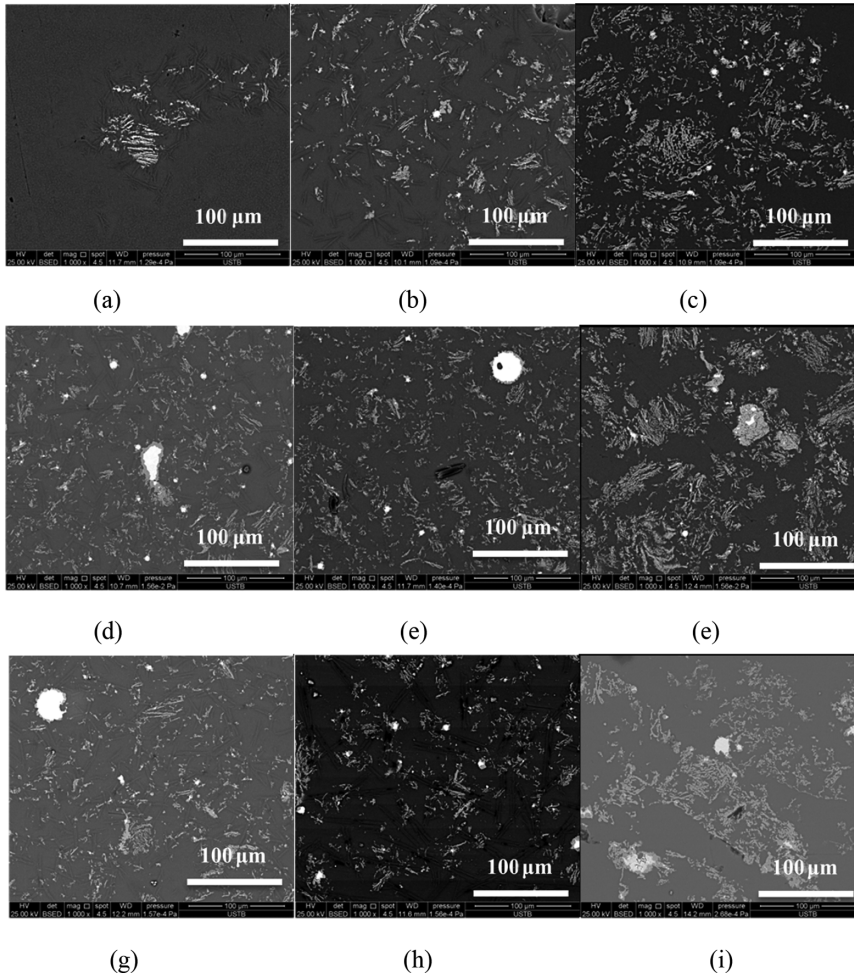


**Figure 18:** BSED images of the samples reduced with different carbon ratios for different times at 1,773 K: (a) 2 h, 0.7; (b) 2 h, 0.85; (c) 2 h, 1.0; (d) 4 h, 0.7; (e) 4 h, 0.85; (f) 4 h, 1.0; (g) 6 h, 0.7; (h) 6 h, 0.85 and (i) 6 h, 1.0.

the areas of TiC phase could be. Therefore, by improving the reaction temperature, the reaction rate and the reduction degree could be accelerated obviously.

- (2) From the experiment results, it was found that TiC had the tendency of concentrating around the iron. Many studies [16–18] pointed that TiC can be chemically wetted in iron, and the wetting angle  $\theta$  between TiC and molten iron is less than  $50^\circ$  even in high temperature and many different kinds of atmosphere. In the slag,  $\text{Fe}_2\text{O}_3$  could be reduced to Fe easily, and then TiC would be heterogeneous nucleation dependence on the iron. Moreover, the grain growth of Fe would be prevented, because of TiC grew around the iron. It may be one reason for the increase of iron loss when more TiC is reduced

during the smelting of  $\text{TiO}_2$  bearing ore in blast furnace.

## Conclusions

The carbothermic reduction process of titanium-bearing blast furnace slag in Panzhihua Iron and Steel Company was investigated in argon atmosphere. Reduction experiments with different carbon ratios at different temperatures for different times were carried out to investigate their influences on the reduction. The following conclusions were obtained:

- (1) The XRD pattern results show that  $\text{MgAl}_2\text{O}_4$  phase disappeared and the main phase of the reduced sample was TiC when the reduction temperature

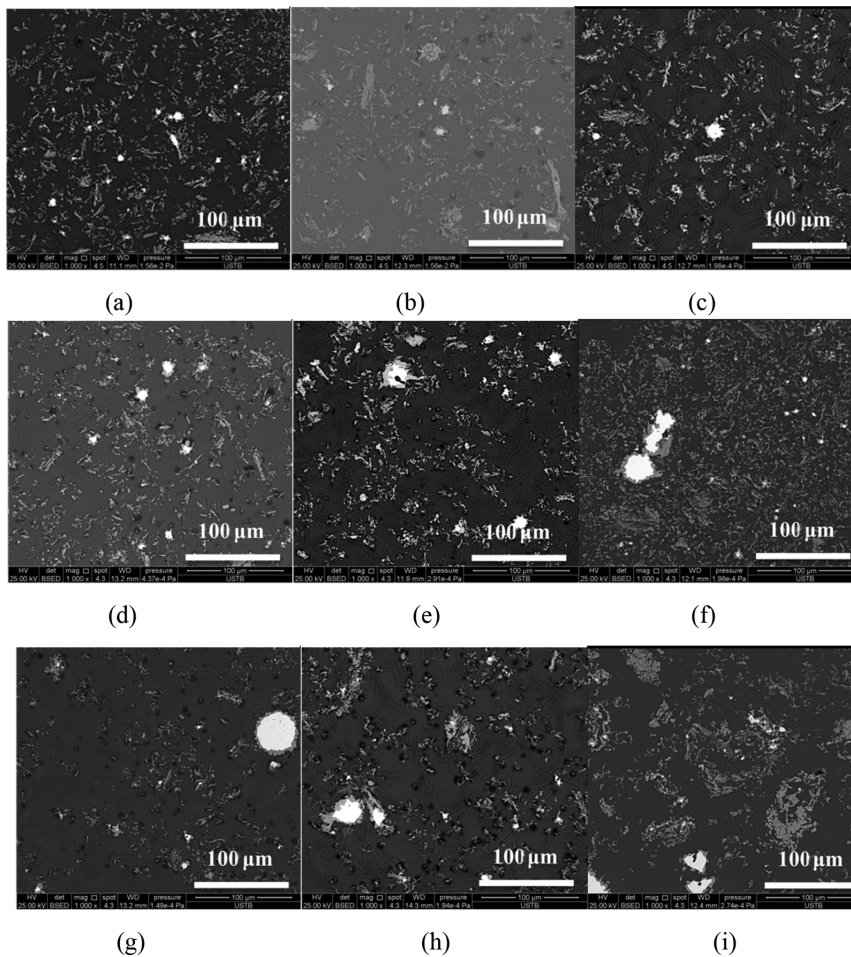


**Figure 19:** BSED images of the samples reduced with different carbon ratios for different times at 1,873 K: (a) 2 h, 0.7; (b) 2 h, 0.85; (c) 2 h, 1.0; (d) 4 h, 0.7; (e) 4 h, 0.85; (f) 4 h, 1.0; (g) 6 h, 0.7; (h) 6 h, 0.85 and (i) 6 h, 1.0.

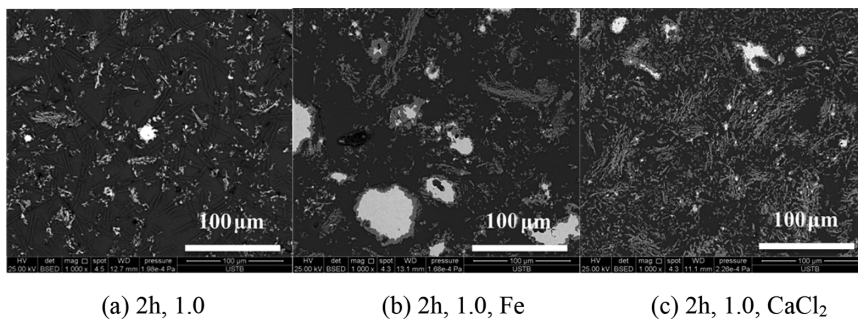


**Figure 20:** BSED images of the samples reduced with carbon ratio of 1.0, 2 h, at 1,873 K for different additives: (a) none; (b) 5 wt% Fe; (c) 5 wt%  $\text{CaCl}_2$ .

was more than 1,773 K. The SEM pictures show that the reduction rate of the titanium-bearing blast furnace slag could be increased by enhancing the temperature and the C content (carbon ratio  $\leq 1.0$ ).

- (2) Fe and TiC were found to be mixed together tightly. TiC would be heterogeneous nucleation on the surface of the iron.
- (3) The additives such as Fe and  $\text{CaCl}_2$  could be helpful for the carbothermic reduction process.



**Funding:** Thanks are given to the financial supports from Specialized Research Fund for the Doctoral Program of Higher Education (20130006120007) and the Fundamental Research Funds for the Central Universities (FTF-TP-14-107A2), as well as the National Natural Science Foundation of China (51174022 and 51474141).

## References

- [1] T. Hu, X. Lv, C. Bai, Z. Lun and G. Qiu, *ISIJ Int.*, 53 (2013) 557–563.
- [2] Z. Yuan, X. Wang, C. Xu, W. Li and M. Kwauk, *Miner. Eng.*, 19 (2006) 975–978.
- [3] C. Li, B. Liang, L.H. Guo and Z.B. Wu, *Miner. Eng.*, 19 (2006) 1430–1438.
- [4] K.S. Coley, B.S. Terry and P. Grieveson, *Metall. Mater. Trans. B*, 26 (1995) 485–494.
- [5] S.K. Gupta, V. Rajakumar and P. Grieveson, *Metall. Trans. B*, 20 (1989) 735–745.
- [6] Y.M. Wang, Z.F. Yuan, Z.C. Guo, Q.Q. Tan, Z.Y. Li and W.Z. Jiang, *T. Nonferr. Metal. Soc.*, 18 (2008) 962–968.
- [7] M.I. El-Guindy and E.G. Davenport, *Metall. Trans.*, 1 (1970) 1729–1734.
- [8] S.K. Gupta, V. Rajakumar and P. Grieveson, *Metall. Trans. B*, 18 (1987) 713–718.
- [9] Y. Zhao and F. Shadman, *AIChE J.*, 36 (1990) 1433–1438.
- [10] D.G. Jones, *J. Appl. Chem. Biotechnol.*, 25 (1975) 561–582.
- [11] K. Sun, R. Takahashi and J.I. Yagi, *ISIJ Int.*, 32 (1992) 496–506.
- [12] C.Y. Li, Y.W. Li, Y.M. Gao, D.B. Yang, Y.B. Li and J.H. Nie, *Iron Steel Vanadium Titanium*, 27 (2006) 5–9.
- [13] Y.M. Gao, C.Y. Li, Y.W. Li, Y.B. Li, J.H. Nie and D.B. Yang, *J. Wuhan Univ. Sci. Technol.*, 30 (2007) 5–9.
- [14] C.J. Feng, J.S. Zhang, *Util. Min. Resour.*, 6 (1997) 34–41.
- [15] H. Li, Y.Q. Qiu, Z.Q. Yang, *J. Univ. Sci. Technol. Beijing*, 18 (1996) 231–235.
- [16] Warren R, *J. Mater. Sci.*, 15 (1980) 2489–2497.
- [17] Dufour LC. *Surface and Interface of Ceramic/Metal Materials*, Kluwer Academic Publisher, London (1989).
- [18] K.Q. Feng, Y. Yang, B.L. Shen, L.B. Guo, *Mater. Des.*, 26 (2005) 37–40.